

DOI: <http://dx.doi.org/10.21123/bsj.2021.18.2.0393>

## Effect of SnO<sub>2</sub>/In<sub>2</sub>O<sub>3</sub> Atomic Ratio on the Structural and Optical Properties of ITO Thin Films

*Zainab Hazim Abdul Raheem*

Department of Physics, College of Science for Women, University of Baghdad, Baghdad, Iraq.

E-mail: [Zainab.h@csw.uobaghdad.edu.iq](mailto:Zainab.h@csw.uobaghdad.edu.iq)

ORCID ID: <https://orcid.org/0000-0001-5869-1703>

Received 22/10/2019, Accepted 10/5/2020, Published Online First 11/1/2021, Published 1/6/2021



This work is licensed under a [Creative Commons Attribution 4.0 International License](https://creativecommons.org/licenses/by/4.0/).

### Abstract:

In this work, the effect of atomic ratio on structural and optical properties of SnO<sub>2</sub>/In<sub>2</sub>O<sub>3</sub> thin films prepared by pulsed laser deposition technique under vacuum and annealed at 573K in air has been studied. Atomic ratios from 0 to 100% have been used. X-ray diffraction analysis has been utilized to study the effect of atomic ratios on the phase change using XRD analyzer and the crystalline size and the lattice strain using Williamson-Hall relationship. It has been found that the ratio of 50% has the lowest crystallite size, which corresponds to the highest strain in the lattice. The energy gap has increased as the atomic ratio of indium oxide increased.

**Key words:** Lattice constants, Lattice strain, Optical Properties, SnO<sub>2</sub>/In<sub>2</sub>O<sub>3</sub>, Structural Properties

### Introduction

The year 1907 was assumed to be the beginning of the discovery of the first transparent conductive oxide, where the cadmium oxide thin film has been prepared using discharge under vacuum and oxidized to get a material of high transparent and good conductivity for first time by Badeker (1). Subsequently, there was a list of potential TCO materials which has been expanded to include such as Al-doped ZnO (2) and indium tin oxide (3) and many others. Today, the most famous transparent conductive oxide is the indium tin oxide (ITO). It is naturally an n-type semiconductor. Indium oxide lattice is doping by tin atoms as cations, doped substations in places and binding with oxygen atoms (4). It has a wide energy gap greater than 3.5 eV, solar cells and many other applications that use transparent conducting layer (5). It is widely used in many optical and electronic devices such as flat-panel displays, gas sensors (6). Indium oxide possesses oxygen vacancies (7) is a material with high electrical conductivity and optical transmittance in the visible range (8). Another possibility to increase the concentration of free electron by doping it by donors such as Sn<sup>4+</sup> (9).

The structural properties of semiconductor materials are important factors affecting their other physical properties such as their electronic properties (10). The amount of impurities might

influence the charge carrier mobility which affects the electrical conductivity, in which the carriers are scattered by grain boundaries and the lattice strain (9). The optical transparency and conductivity of the ITO films are highly affected by reducing its grain size. The small grain sizes improve the uniformity, and hence improving thin film properties (11).

The aim of this work is to study the effect of atomic ratio of SnO<sub>2</sub>/In<sub>2</sub>O<sub>3</sub> thin films synthesized by pulsed laser deposition and annealed at 573 K on crystallite size and lattice strain and optical properties of the composite.

### Materials and method:

Tin oxide powder (SnO<sub>2</sub>) of (99.9 %) purity and indium oxide (In<sub>2</sub>O<sub>3</sub>) of (99.998% %) purity, from Sigma-Aldrich, have been mixed as molar ratios of (0:100, 25:75, 50:50, 75:25 and 100:0) by ball mill and pressed in mold of 1.5cm diameter. The composite thin films have been prepared on glass substrates under vacuum of 10<sup>-3</sup> mbar by Nd:YAG pulsed laser of 1064 nm wavelength, and has 800 mJ pulse energy, 9 nanosecond pulse duration and 6 Hz repetition frequency as shown in Fig1. The rotated substrate is placed parallel to target surface at 2 cm separation distance. The deposited films have been annealed at 573 K for 1 hour in the air. Thin film thickness was measured

using a reflectivity spectrometer model (TF Probe TM / Angstrom Sun Technology Inc.), about  $200 \pm 10$  nm for all samples. The final films have been examined by x-ray diffraction from Shimadzu. The crystalline size and lattice strain have been determined to utilize the peaks broadening using Williamson-Hall analyzing method. The optical properties of the pure and composite films of different ratios have been studied in the range of 300–1100 nm using UV-Visible spectrometer.

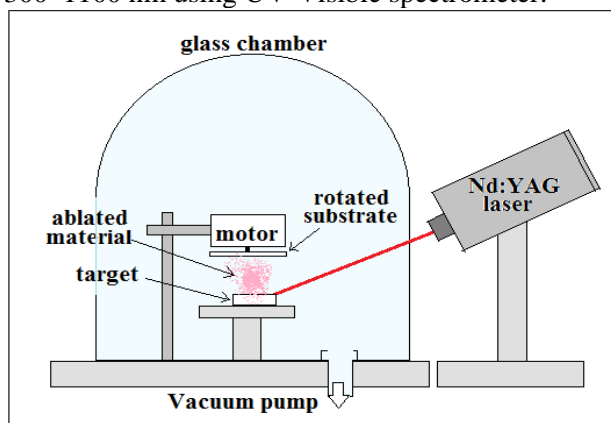


Figure 1. Thin films deposition setup.

## Results and Discussions:

Figure 2 illustrates the x-ray diffraction patterns of the tin oxide, indium oxide and their mixed films prepared by pulsed laser deposition technique (PLD) and annealed at 573 K. All thin films have polycrystalline structure. The x-ray diffraction pattern for pure  $\text{SnO}_2$  film has four peaks located at  $26.48^\circ$ ,  $33.68^\circ$ ,  $37.74^\circ$  and  $51.38^\circ$  corresponding to (110), (101), (200) and (111) directions respectively. These peaks agree with the standard card (96-210-4744) (12).

The X-ray diffraction pattern for  $\text{In}_2\text{O}_3$  films illustrates polycrystalline structure with peaks located at  $21.52^\circ$ ,  $30.50^\circ$ ,  $35.28^\circ$ ,  $45.54^\circ$ ,  $50.70^\circ$ ,  $60.22^\circ$  and  $63.14^\circ$  belong to the (211), (222), (111), (400), (440), (622) and (444) directions respectively of good agreement with the standard card (96-101-0589) of  $\text{In}_2\text{O}_3$  lattice. The comparison between samples with different  $\text{In}_2\text{O}_3/\text{SnO}_2$  ratios illustrates that the increasing of  $\text{In}_2\text{O}_3$  ratio leads to increase the in peaks intensities and decrease the intense of  $\text{SnO}_2$  peaks and completely disappeared at the ratio of 0.75 ratio, this indicates that all tin ions are contained in the indium oxide lattice. The crystallinity has been increased as the ratio of  $\text{In}_2\text{O}_3$  increased due to the increasing of peaks intensities. This result is in agreement with Mei *et al.* (13).

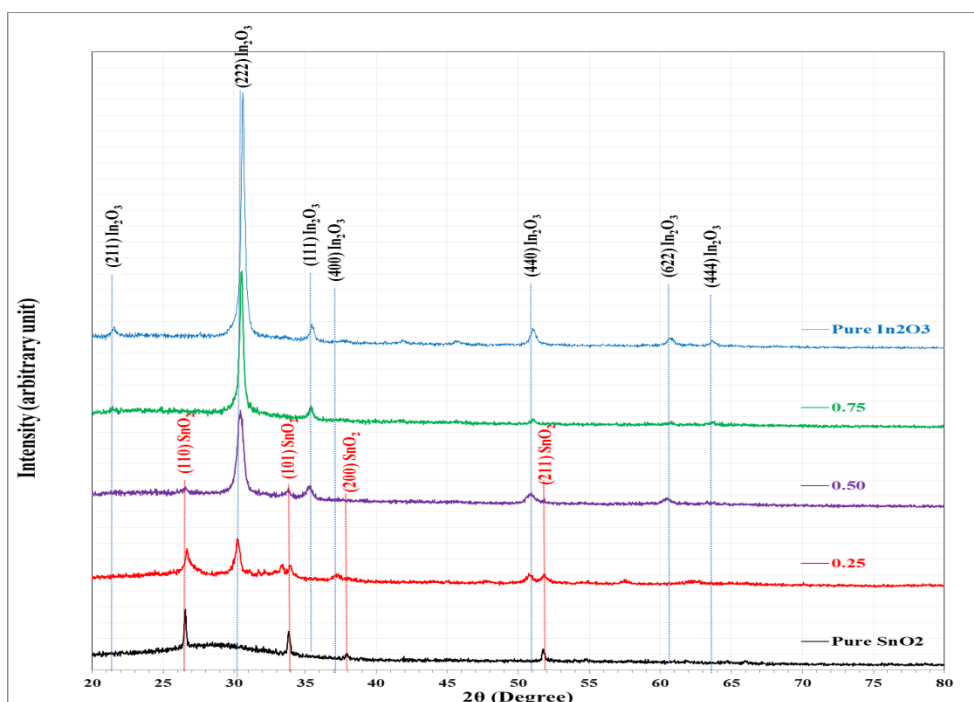


Figure 2. XRD patterns of  $\text{SnO}_2$ ,  $\text{In}_2\text{O}_3$  and their composite films prepared at different ratios.

Figure 3 shows the 2D XRD patterns corresponding to the composite ratio. It is imaging of the phase conversion point. It is clearly that the major phase of the sample of 25%  $\text{In}_2\text{O}_3/\text{SnO}_2$  is due to the cubic  $\text{In}_2\text{O}_3$  crystal phase. The increasing

of the ratio up to 100% causes a shifting in the intensities of the preferred peak (222) to higher values as shown in Fig. 4 indicates the decreasing in the interatomic distance ( $d_{hkl}$ ) due to the reduced lattice constant as the variation of lattice strain.

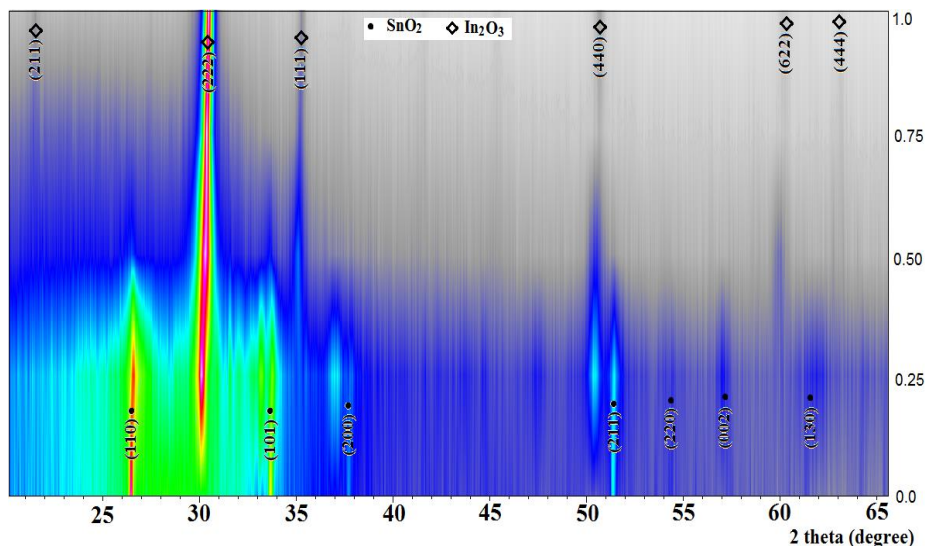


Figure 3. 2D X-ray diffraction phase variation plot for SnO<sub>2</sub>/In<sub>2</sub>O<sub>3</sub> thin films at different ratios.

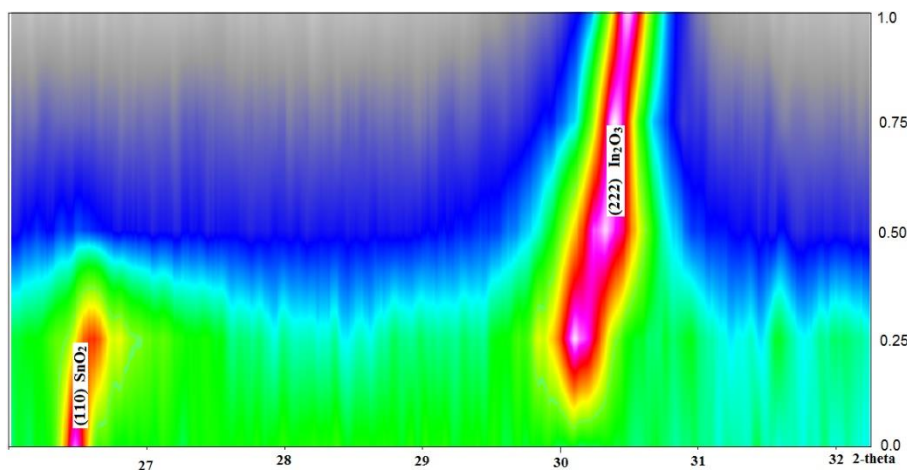


Figure 4. (110) SnO<sub>2</sub> and (222) In<sub>2</sub>O<sub>3</sub> peaks variation according to composite ratio.

Figure 5 shows the planes of preferred orientation of indium oxide (222) and tin oxide (110) (formed by Diamond software), the density of atoms per unit area of (222) plane in indium oxide is large, compared to those in tin oxide (110)

where the density per unit area is low. This leads to increase in the X-ray diffraction at (222) plane, which causes a higher intensity even in the lower ratio of indium oxide.

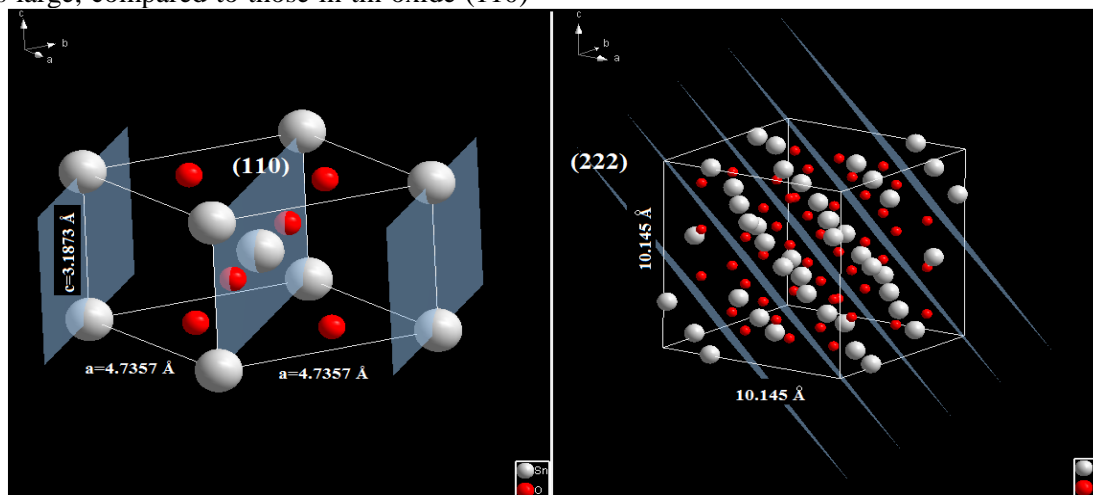


Figure 5. Planes of preferred orientation for tetragonal SnO<sub>2</sub> and cubic In<sub>2</sub>O<sub>3</sub> by diamond software (14) according to data from standard card no. 96-210-4744 and 96-101-0589 respectively.

The lattice constant (*a*) for the cubic structure has been calculated using the interatomic distance, calculated from the Bragg angle ( $2\theta$ ) of the preferred orientation peak according to  $a = \sqrt{h^2+k^2+l^2}d_{hkl}$ . It is clear that the lattice

constant has been decreased from 10.27 Å to 10.145 Å compared with the lattice constants of pure SnO<sub>2</sub> of (*a*= 4.736 Å and *c*= 3.187 Å) with increasing In<sub>2</sub>O<sub>3</sub> ratio from 25 to 100% as shown in Fig. 6 due to the difference between indium and tin ion radius.

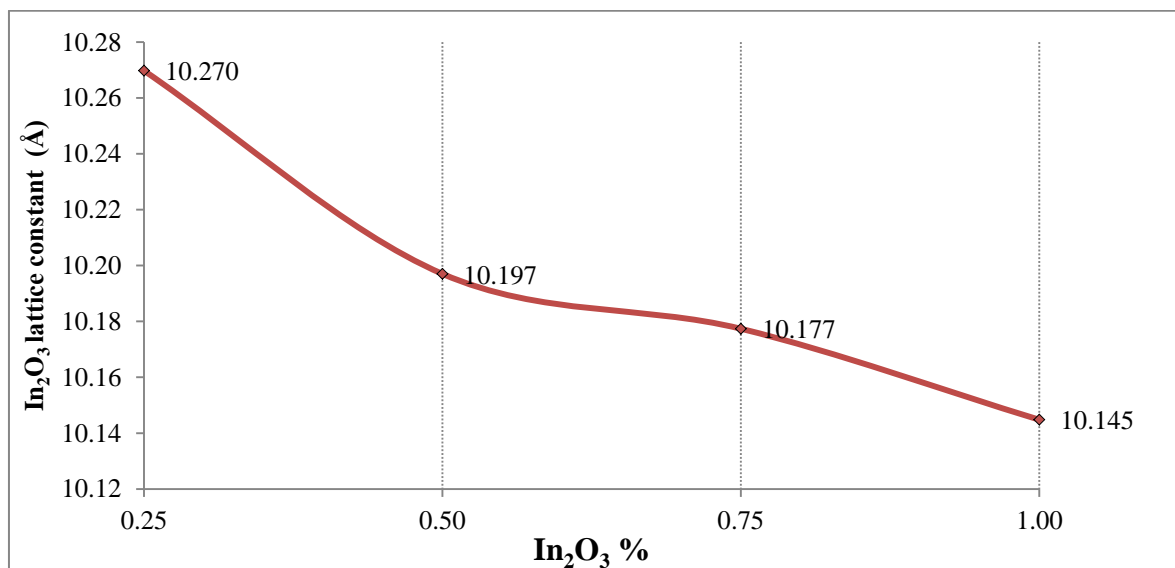


Figure 6. Variation of lattice constant (*a*) for In<sub>2</sub>O<sub>3</sub> with composite ratio.

The line broadening of x-ray diffraction peaks in the form of Cauchy distribution is due to crystal size effect and lattice strain, which are two independent variables. The line width at half maximum ( $\beta_{hkl}$ ) is the sum of the two broadening effects which have been calculated using the Debye-Scherrer formula and the broadening has been caused by the lattice strain (15)

$$\beta_{hkl} = \frac{k\lambda}{L \cos\theta} + 4 \varepsilon \tan\theta \quad \dots\dots\dots 1$$

Where *k* is the shape factor which is equal to 0.94 for cubic crystals, *L* is the crystallite size,  $\lambda$  is the x-

ray wavelength,  $\theta$  is the Bragg angle and  $\varepsilon$  is the strain in lattice

By rearranging the above equation, one get (16)

$$\beta_{hkl} \cos\theta = \frac{k\lambda}{L} + 4 \varepsilon \sin\theta \quad \dots\dots\dots 2$$

Williamson-Hall plot is the plot of  $\beta_{hkl} \cos\theta$  against  $4 \sin\theta$ . Utilizing the best linear fit, the crystalline size has been determined from the y-intercept, and the slope of the line equivalent of the non-uniform strain ( $\varepsilon$ ). The strain in lattice and domain crystallite size of prepared SnO<sub>2</sub>/In<sub>2</sub>O<sub>3</sub> thin films at different atomic ratios, have been calculated using Williamson-Hall plot, as shown in Fig. 7.

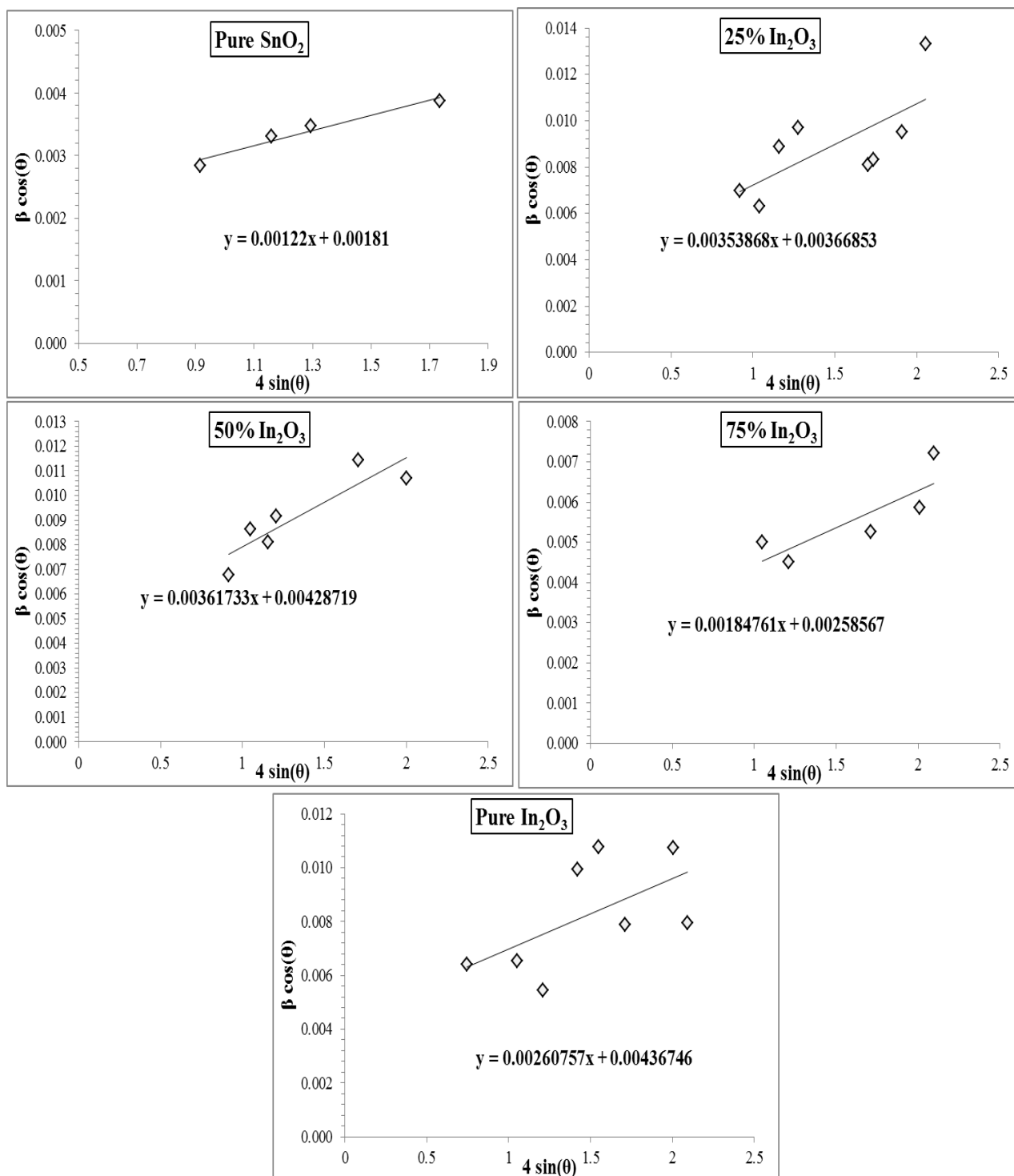


Figure 7. Williamson - Hall plot the pure and composite samples at different ratios.

The calculated strain and crystalline size values have been compared with  $\text{In}_2\text{O}_3$  atomic ratio in Fig.8. It is noted that the crystalline size has a minimum value (32.4 nm) at the 50%  $\text{In}_2\text{O}_3/\text{SnO}_2$

ratio and has been increased with increasing the ratio. While, the lattice strain has convenient behavior with maximum value of 0.00579 at the same ratio, as shown in Fig. 8.

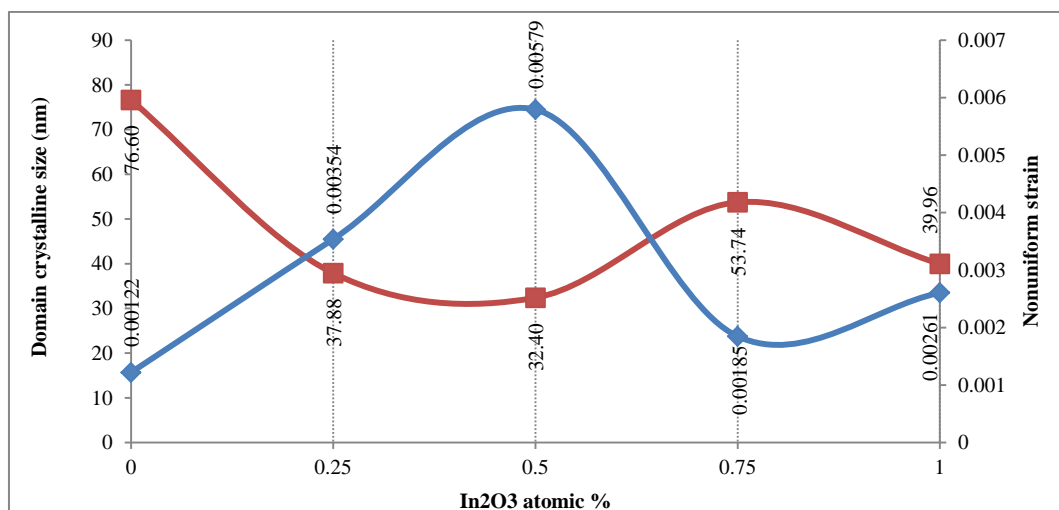


Figure 8. Domain crystalline size and non-uniform strain of SnO<sub>2</sub>/In<sub>2</sub>O<sub>3</sub> composite thin films at different ratios.

The correlation between non-uniform strain and average crystallite size is shown in Fig.9. It is observed that the particles with large average size have less strain, which indicates that high

crystallinity can be reduced the lattice strain (17). However, the samples with particle size below 40 nm have characteristic strain due to the small size effect, as shown in Fig.9.

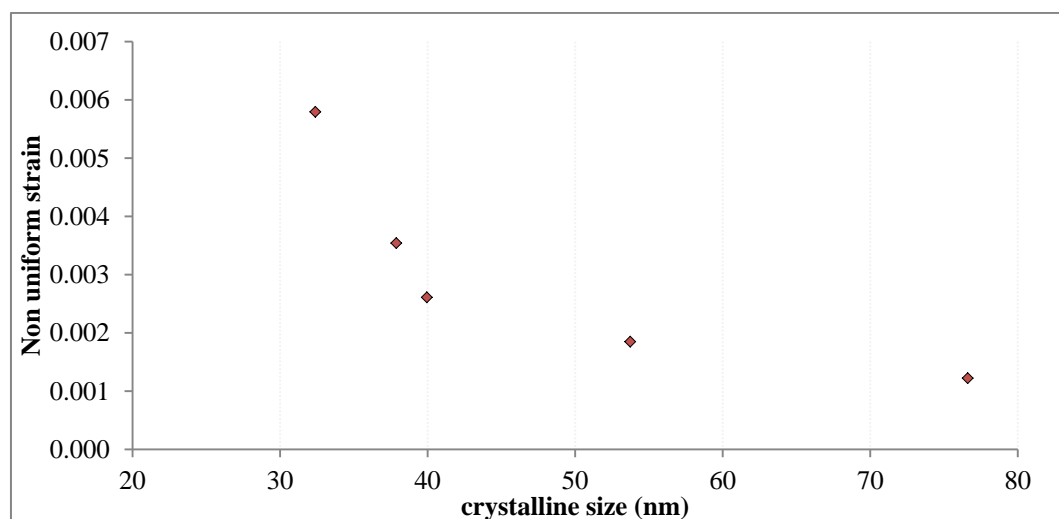


Figure 9. The plot of lattice strain as a function of crystallite size

Figure 10 shows transmission patterns of the pure and SnO<sub>2</sub>/In<sub>2</sub>O<sub>3</sub> thin films of 200 nm thickness prepared at different atomic ratios. The transmittance spectrum has been increased as the ratio of composite increasing (the transmission at 500 nm has been increased from 70 to 92% with

increasing In<sub>2</sub>O<sub>3</sub> ratio from 0 to 100%). There is a sharp fall in the transmission curves especially for In<sub>2</sub>O<sub>3</sub> thin film sample due to high crystallinity and the reduction of the tail states near the absorption edge (18).

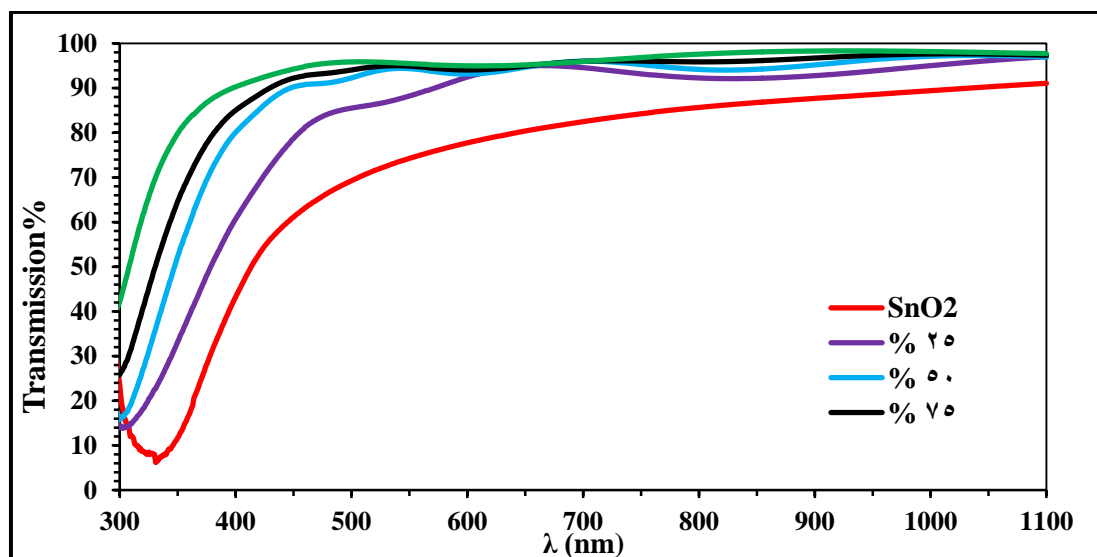


Figure 10. Transmission spectra of SnO<sub>2</sub>/In<sub>2</sub>O<sub>3</sub> thin films of 200 nm thickness prepared at different atomic ratios.

The optical energy gap values ( $E_g^{opt}$ ) for the pure and composite samples have been determined using Tauc equation for allowed direct transition

shown in Fig. 11. It is clearly that  $E_g^{opt}$  has been increased as the atomic ratio of In<sub>2</sub>O<sub>3</sub> increasing. This result agrees with Klein et al (19).

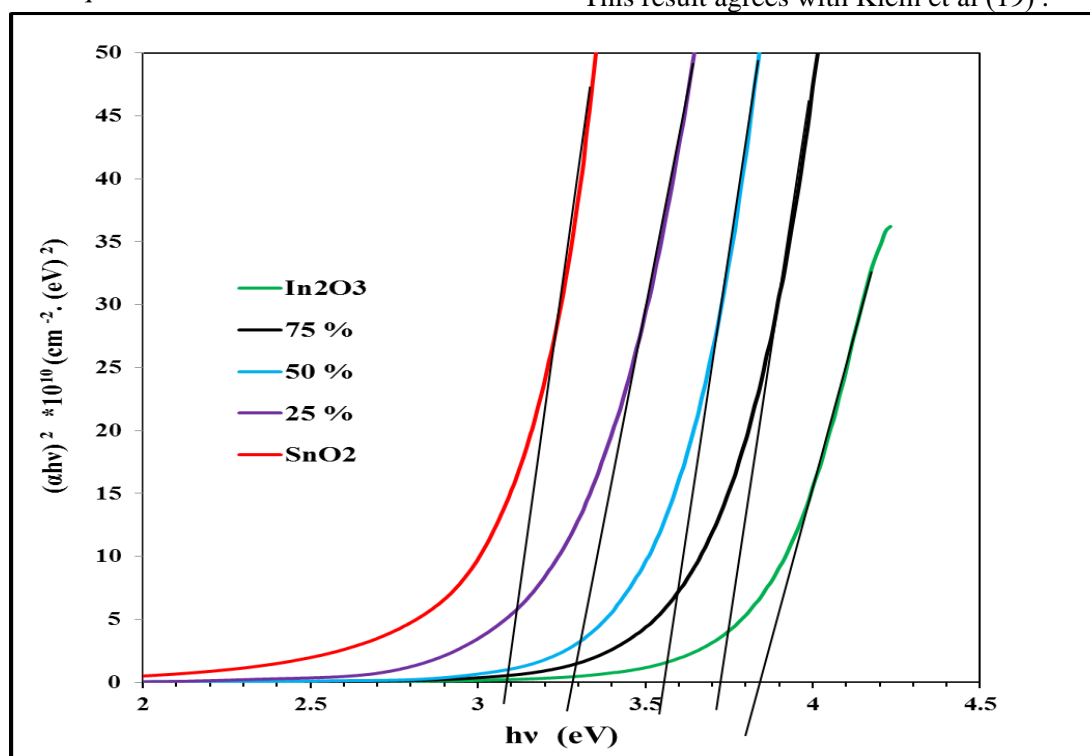


Figure 11.  $(\alpha h\nu)^2$  vs.  $(h\nu)$  for SnO<sub>2</sub>, In<sub>2</sub>O<sub>3</sub> and their composite films of different atomic ratios.

### Conclusions:

SnO<sub>2</sub>/In<sub>2</sub>O<sub>3</sub> thin films have been prepared in different atomic ratio by pulsed laser deposition under vacuum. The structural properties studied show that the indium oxide is a cubic phase even in small atomic ratio. The domain crystalline size has been changed as the atomic ratio changed and the smallest crystalline size is found at an atomic ratio of 50% due to the highest non-uniform strain in the

lattice (the decreasing of the crystallite size may be cause more lattice strain). The optical energy gap has been increased with increasing the atomic ratio of indium oxide.

### Author's declaration:

- Conflicts of Interest: None.
- I hereby confirm that all the Figures and Tables in the manuscript are mine. Besides, the Figures

and images, which are not mine, have been given the permission for re-publication attached with the manuscript.

- Ethical Clearance: The project was approved by the local ethical committee in University of Baghdad.

## References:

1. Badeker K. Uber die elehtrische Leitfiihigkeit Und die. Thermoelektrische Krafteiniger Schwermetallverbindungen. Ann Phys. 1907; 19: 749-750 ..
2. Jannanea T, Manoua M, Liba A, Fazouan N, El Hichou A, Almaggoussi A. Sol-gel Aluminum-doped ZnO thin films: Synthesis and characterization. J Mater Environ Sci. 2017;8(1):160–168.
3. Bel-hadj-tahar R, Mohamed AB. Sol-Gel Processed Indium-Doped Zinc Oxide Thin Films and Their Electrical and Optical Properties. NJGC. 2014;4:55–65.
4. Joseph J, Ramamurthy S, Subramanian B, Sanjeeviraja C, Jayachandran M. Spray pyrolysis growth and material properties of In<sub>2</sub>O<sub>3</sub> films. J Cryst Growth. 2002; 240(1–2):142–151.
5. Hasan BA, Abdallah RM. The role of Tin Oxide Concentration on The X-ray Diffraction, Morphology and Optical Properties of In<sub>2</sub>O<sub>3</sub>:SnO<sub>2</sub> Thin Films J Phys. 2018;1003:012129.
6. Shariati M, Khosravinejad F. The Laser-Assisted Field Effect Transistor Gas Sensor Based on Morphological Zinc-Excited. Surf Rev Lett. 2017;24(8):1–11.
7. Nirmala E, Punithavathy IK, Jeyakumar SJ. Analysis on O<sub>3</sub> sensing and conducting property of Sn doped In<sub>2</sub>O<sub>3</sub> using hydrothermal preparation method. J Appl Sci Eng. Methodol. 2016;2(3):371–375.
8. Tuna O, Selamet Y, Aygun G, Ozyuzer L. High quality ITO thin films grown by dc and RF sputtering without oxygen. J Phys D Appl Phys. 2010;43(5):055402-7.
9. Abe R, Fujishiro H, Naito T. Substitution effect of tetravalent and pentavalent elements on thermoelectric properties in In<sub>2</sub>O<sub>3</sub>-SnO<sub>2</sub> system. Trans Mat Res Soc. Japan. 2016;41(1):101–108.
10. Ge W, Chang Y, Natarajan V, Feng Z, Zhan J. In<sub>2</sub>O<sub>3</sub>-SnO<sub>2</sub> hybrid porous nanostructures delivering enhanced formaldehyde sensing performance. J Alloys Compd. 2018;746:36–44.
11. Xu J, Yang Z, Zhang X, Wang H, Xu H. Grain size control in ITO targets and its effect on electrical and optical properties of deposited ITO films. J Mater Sci Mater Electron. 2014; 25(2):710–716.
12. Peng L, Xiao Y, Wang X, Feng D, Yu H, Dong X. Realization of Visible Light Photocatalysis by Wide Band Gap Pure SnO<sub>2</sub> and Study of In<sub>2</sub>O<sub>3</sub> Sensitization Porous SnO<sub>2</sub> Photolysis Catalyst. Chemistry Select. 2019;4(29):8460–8469.
13. Mei F, Yuan T, Li R, Zhou L, Qin K. Effects of particle size and dispersion methods of In<sub>2</sub>O<sub>3</sub>-SnO<sub>2</sub> mixed powders on the sintering properties of indium tin oxide ceramics. Int J Appl Ceram Technol. 2018;15(1):89–100.
14. Diamond.4.6.1 software for Scientists, Crystal Impact co. 2019. Bonn, Germany
15. Ighodalo KO, Obi D, Agbogu A, Ezealigo BN, Nwanya AC, Mammah SL, et al. The Structural and Optical Properties of Metallic doped Copper (I) Iodide Thin Films Synthesized by SILAR Method.. Mater Res Bull. 2017;94:528–536.
16. Thirumoorthi M, Joseph JT. Structure, optical and electrical properties of indium tin oxide ultra thin films prepared by jet nebulizer spray pyrolysis technique. J Asian Ceram Soc. 2016; 4(1):124-132.
17. Kurian M , Kunjachan C. Investigation of size dependency on lattice strain of nanoceria particles synthesised by wet chemical methods.Int Nano Lett. 2014; 4:73–80.
18. Koole R, Groeneveld E, Vanmaekelbergh D. Nanoparticles-Workhorses of nanoscience. Springer-Verlag Berlin Heidelberg, 1<sup>st</sup> edition, Ch1, 2014.
19. Klein A, Körber C, Wachau A, Sauberlich F, Gassenbauer Y, Harvey SP, et al. Transparent Conducting Oxides for Photovoltaics: Manipulation of Fermi Level, Work Function and Energy Band Alignment. Materials . 2010;3:4892–4914.

## تأثير النسبة الذرية SnO<sub>2</sub>/In<sub>2</sub>O<sub>3</sub> على الخواص التركيبية والبصرية لأغشية ITO الرقيقة

زينب حازم عبد الرحيم

قسم الفيزياء، كلية العلوم للبنات، جامعة بغداد، بغداد، العراق.

### الخلاصة:

تم في هذا العمل دراسة تأثير النسبة الذرية على الخواص التركيبية والبصرية لأغشية مزيج اوكسيد الانديوم/اوكسيد القصدير المحضر بطريقة الليزر النبضي في الفراغ، ثم التلدين عند 573 كلفن في الهواء. تم تحليل العينات بنسب ذرية من 0 الى 100 % باستخدام حيود الاشعة السينية لدراسة تأثير النسب على تغير الطور الناتج باستخدام التحليل تغير الطور لحيود الاشعة السينية و دراسة الحجم البلوري و الاجهادات في الشبكة باستخدام علاقة وليامسون-هول. وجد ان النسبة ٥٠% تكون ذات اقل حجم حبيبي والتي تقابل اعلى اجهاد في الشبكة. كذلك تم دراسة تأثير النسبة على الخصائص البصرية حيث وجد ان فجوة الطاقة تزداد بزيادة النسبة الذرية لأوكسيد الانديوم.

الكلمات المفتاحية: ثابت الشبكة، جهد الشبكة، الخواص البصرية، اوكسيد الانديوم:اوكسيد القصدير، الخواص التركيبية.